

interphase film on the mesophase carbon microbead anode surface.¹⁴ Plenty of previous studies have shown sulfone solvents or additives are useful to improve electrochemical stability of the LIBs.^{15–17} However, there are still some limitations because of the high viscosity of sulfone-based electrolytes.^{18–20}

Recently, theoretical calculations have been increasingly applied in designing the electrolytes system for LIBs.^{21,22} Through comprehensive quantum chemistry (QC) calculations using classical theories and well-benchmarked molecular dynamics, covering lithium salt anions and solvents with a broad range in chemistry, systematic correlations can be elucidated between molecular level interactions and composite electrolyte properties, such as electrochemical stability and solvent structures.²³ Besides, QC calculations are employed to gain insight into the mechanisms of the observed coatings' formation.²⁴ Theoretically, frontier molecular orbital theory suggests that the stability of a solvent mainly results from the ability of gaining or losing electrons for a solvent molecule. The electron-accepting and -donating capability of the solvent molecules, as well as the spatial orientation of reactions between molecules and other properties, are dependent on frontier molecular orbitals, including the highest occupied molecular orbital (HOMO) and the lowest unoccupied molecular orbital (LUMO). Usually, a practical lithium-ion battery requests that the electrochemical potential (EP) of the anode is lower than the LUMO of the electrolyte and the EP of the cathode is higher than the HOMO of the electrolyte.²⁵ In general, the lower the HOMO energy, the better the oxidation resistance presents; and the higher the LUMO energy, the better the reduction resistance. As a result, with regard to high-voltage electrolytes, the HOMO energy of the electrolyte components should be as low as possible. The main factors that affect the electrochemical stability of the solvent are polar functional groups contained in the solvent, such as carbonyl group (C=O), sulfone (–SO₂–), and ether (–O–) group. In addition, the structural factors of the solvents also have great influence on the stability of the electrolyte, including electronic effects and steric effects, which can be analyzed by attenuated total internal reflectance Fourier transform infrared spectroscopy (ATR-FTIR).

On the basis of the above-mentioned considerations, we have compared some sulfones that possess desired electrochemical stability by QC calculations and chose favorable sulfones as solvents as well as suitable sulfites as cosolvents to adjust the viscosity of solvents. Furthermore, the electrochemical properties of the as-designed cosolvents are tested to verify the simulated results, and the possible interactions between lithium salts and sulfone solvents are analyzed by ATR-FTIR, thus enabling the LIBs to obtain the high-voltage characteristics.

2. EXPERIMENTAL SECTION

2.1. Theoretical Calculations. Quantum chemical calculations were completed through density functional theory (DFT). The theoretical calculations were performed using Gaussian 09 program package.²⁶ And the DFT method was used with Becke's three-parameter (B3) exchange functional together with Lee–Yang–Parr (LYP) nonlocal correlation functional (B3LYP). All complexes were treated at B3LYP/6-31+G(d, p) level for full geometry optimization. 6-31+G is one set of diffuse s and p functions on heavy atoms, which presents good reproducibility of both ion pairs and anodic oxidation–reduction potential. Specifically, all of the potential energy surface structures are optimized at a local minimum without imaginary frequency.

2.2. Preparation of High-Voltage Electrolytes. To constitute high-voltage electrolytes, the following sulfones were purchased and used as received: tetramethylene sulfone [C₄H₈O₂S] (TMS; Acros), ethyl methyl sulfone [C₂H₅SO₂CH₃] (EMS; TCI), ethyl vinyl sulfone [C₂H₅SO₂C₂H₃] (EVS; Aldrich), dimethyl sulfite [C₂H₆O₃S] (DMS; Acros), and diethyl sulfite [C₄H₁₀O₃S] (DES; Adamas). Three lithium salts were purchased as well: lithium bis(oxalate)borate (LiBOB; Acros), bis(trifluoromethane) sulfonimide lithium salt (LiTFSI; Acros), and lithium hexafluorophosphate (LiPF₆; Acros).

Equal quantities of TMS and DMS and TMS and DES were mixed in isotope flasks and then certain amounts of three different lithium salts: LiPF₆, LiBOB, and LiTFSI were slowly added into the flask, respectively, with continuous stirring, until the mixtures turned into transparent solutions. The concentrations of lithium salts in TMS/DMS (or TMS/DES) varied from 0.4 to 1.8 mol/L. All the operations were performed in a glovebox (Mbraun) filled with argon.

2.3. Characterizations of Sulfone-Based High-Voltage Electrolytes. The electrochemical windows of all sulfone-based electrolytes were measured in a reformative three-electrode system, where a platinum microelectrode was used as the working electrode and lithium sheet was used as both the counter electrode and reference electrode. The cyclic voltammograms were recorded at a scan rate of 1 mV s^{–1} in the scan range from –1.0 to 7.0 V.

Ionic conductivities of the sulfone-based electrolytes were measured by electrochemical impedance spectroscopy. The impedance of the Pt/sulfone-based electrolytes/Pt was tested at a temperature ranging from –20 to 60 °C in an argon atmosphere.

The FTIR spectra of the samples, which were placed on the ATR unit in the glovebox, were recorded on a NICOLET6700 spectrometer at 4000–500 cm^{–1} in an argon atmosphere, and the spectral resolution was 2 cm^{–1}.

3. RESULTS AND DISCUSSION

3.1. Molecular Frontier Orbitals of Sulfone Molecules.

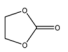
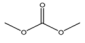
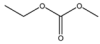
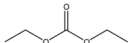
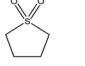
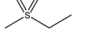
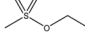
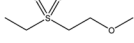
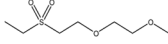
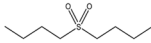
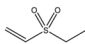
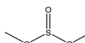
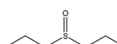
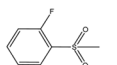
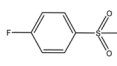
Frontier molecular orbital theory implies that the abilities of oxidation and reduction resistance have a certain relationship with the molecule's HOMO energies²² since during oxidation the molecule of electrolyte loses one electron from its HOMO. Both HOMO and LUMO energies have been calculated using Gaussian09 with Gaussview software package, and the calculation results of typical carbonates and sulfone solvents using the DFT method are listed in Table 1.

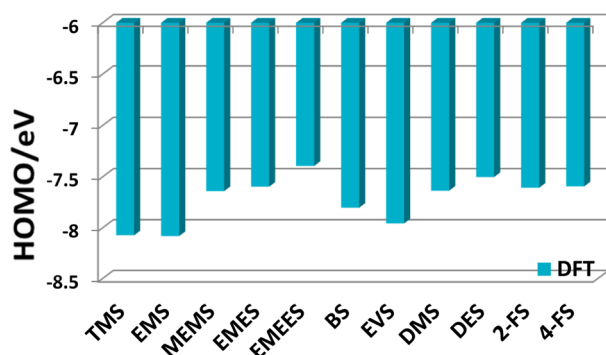
The main advantage of DFT is that it can provide an economical route to compute the properties of large molecules accurately. And for a system with strong intermolecular force, the DFT even provides a more suitable way to predict the molecular properties.^{27,28}

As can be seen in Table 1, the values of the HOMO energies for typical carbonates used as solvents such as EC, DMC, EMC (ethyl methyl carbonate), and DEC (diethyl carbonate) present a tendency from low to high as EC < DMC < EMC < DEC. Namely, the EC exhibits the best antioxidant capacity among these four solvents and then comes DMC, EMC, and DEC. This result matches perfectly with the previous calculations research.²⁹

It is reasonable to note that the QC calculation is a powerful tool to investigate the antioxidant capacities of the sulfone solvents. To make the calculation results of the HOMO energies more visually oriented, Figure 1 shows the values of the HOMO energies for sulfone solvents presenting a tendency as EMS < TMS < EVS < BS (butyl sulfone) < MEMS (methoxyethylmethyl sulfone) < DMS < 2-FS [1-fluoro-2-(methyl-sulfonyl)benzene] < EMES (ethylmethoxyethyl sulfone) < 4-FS [4-fluoro-2-(methyl-sulfonyl)benzene] < DES < EMEES (ethylmethoxyethoxyethyl sulfone). It indicates that

Table 1. Frontier Molecular Orbitals of Carbonates and Sulfones Used as Electrolyte Solvents Using Geometry Optimization (Simulated at the DFT/6-31+G(d,p) Level)

Solvent	Name	Structure	$E_{\text{HOMO}}/\text{eV}$	$E_{\text{LUMO}}/\text{eV}$
EC	Ethylene Carbonate		-8.468	-0.604
DMC	Dimethyl Carbonate		-8.179	-0.370
EMC	Ethyl Methyl Carbonate		-8.133	-0.256
DEC	Diethyl Carbonate		-8.055	-0.268
TMS	Tetramethylene sulfone		-8.074	-0.694
EMS	Ethyl Methyl Sulfone		-8.082	-0.622
MEMS	Methoxyethyl Methyl Sulfone		-7.639	-0.516
EMES	Ethylmethoxy Ethyl Sulfone		-7.596	-0.527
EMEES	Ethylmethoxy Ethoxyethyl Sulfone		-7.394	-0.546
BS	Butyl Sulfone		-7.802	-0.513
EVS	Ethyl Vinyl Sulfone		-7.957	-1.558
DMS	Dimethyl Sulfoxide		-7.635	-0.952
DES	Diethyl Sulfoxide		-7.502	-0.773
2-FS	1-Fluoro-2-(methyl-sulfonyl) benzene		-7.606	-1.646
4-FS	4-Fluoro-2-(methyl-sulfonyl) benzene		-7.592	-1.499

**Figure 1.** HOMO energies of typical sulfone-based solvents (calculated at the DFT/6-31+G(d,p) level).

the antioxidant capacities of these sulfone solvents are in the converse order.

As shown in Figure 1, TMS, EMS, EVS, and some linear sulfones derived from EMS such as MEMS, EMES, and EMEES display relatively low HOMO energies and their oxidation

resistance abilities may be satisfying. It is notable that for the linear sulfones, such as EMS, TMS, and EVS, the oxidation reactions often occur in a sulfone group, whereas for the ether sulfones, the oxidation reactions usually happen on the ether group. For the linear sulfones derived from EMS, with an increase of the carbon chain length and the number of ether groups, the HOMO energy shows rising trends as well; thus, the oxidation resistance will be worse. The reason is that the ether group $-\text{O}-$ is more easily oxidized than the sulfone group $\text{O}=\text{S}=\text{O}$ in these linear sulfone solvents, and such functional effect of the ether group probably reduces the oxidation potential of the whole molecule.

According to the above analysis, sulfones with low HOMO energies and good ionic conductivities possibly have favorable electrochemical performance. As for some suitably designed high-voltage electrolyte solvents, the QC calculation is an efficient way to make some predictions on the oxidation or reduction stability of solvents. It can also provide some detailed information on the molecules, such as which group in a sulfone molecule plays the key role, or if there are some other structural factors that would influence the properties.

However, the sulfone compounds still show some weaknesses when practically used in LIBs. Generally, most of the sulfones have high melting points and high viscosities; thus, it cannot be used solely in LIBs. To solve this problem, here we combined the sulfones that have high dielectric constants and high viscosities with those sulfones that have low dielectric constants and low viscosities, to form a composite electrolyte system. Considering both DMS and DES have similar structures and low viscosities (shown in Table 2), we first

Table 2. Physical and Chemical Parameters of Typical Carbonate Solvents and Sulfones (25 °C)

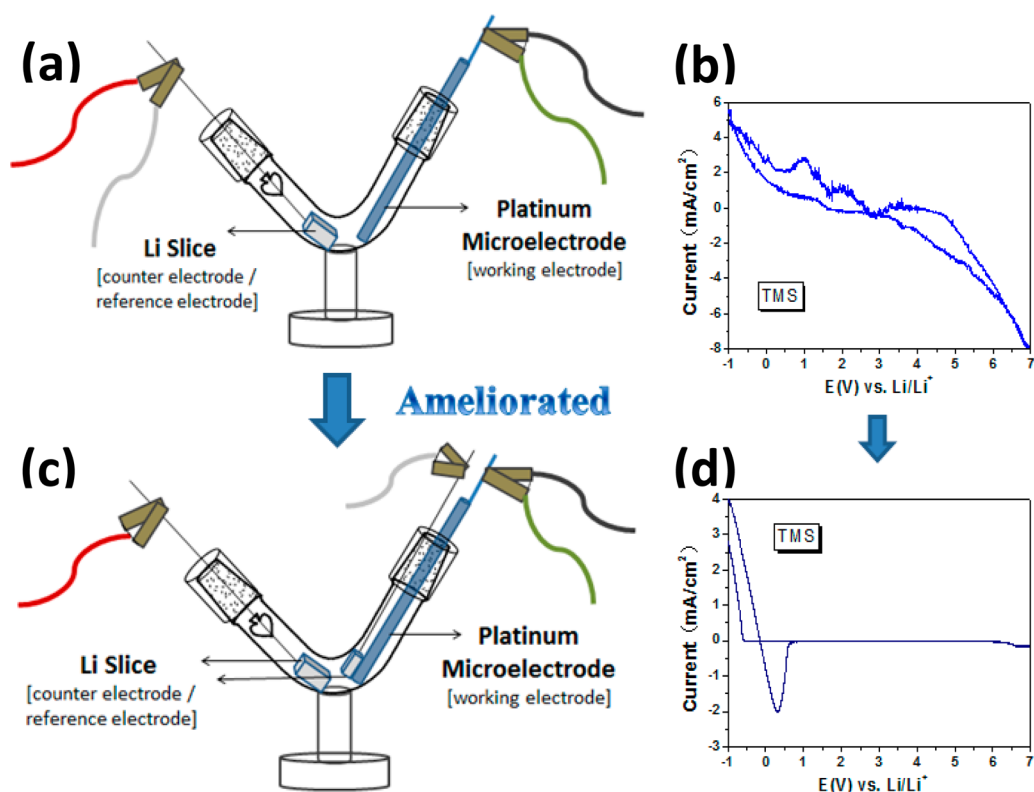
solvent	melting point (°C)	flash point (°C)	boiling point (°C)	viscosity (cp)	dielectric constant
EC	37	160	238	1.85	89.6
DEC	-43	25	127	0.75	2.82
DMC	3	17	90	0.625	2.6
TMS	26	166	285	10.34	44
DMS	-141	30	126	0.87	22.5
DES	-112	53	159	0.83	15.6
EMS	34	34	184		
EVS		112	237		

select DMS to adjust the viscosities of EMS, TMS, and EVS, and then TMS was selected to be the main solvent with DMS or DES, added with various lithium salts, to research further the electrochemical properties of the sulfone electrolytes.

3.2. Electrochemical Stabilities of Sulfone Electrolytes. Physical and chemical parameters of typical organic solvents and sulfones are listed in Table 2.

The electrochemical stabilities of several sulfone-based electrolytes were investigated by cyclic voltammetry (CV). First, several sulfone solvents were mixed with the cosolvent DMS and then added with LiTFSI to form electrolytes. All of the as-prepared electrolytes were tested in a reformative three-electrode system, as is shown in Scheme 1. This device uses a V-shape glass container to hold a small amount of electrolytes, where the counter electrode and the reference electrode are separated (Scheme 1c), when being compared with the two-electrode system using one piece of lithium serves as both the counter and the reference electrodes (Scheme 1a).

Scheme 1. Comparison of Three- and Two-Electrode Devices for Testing Electrochemical Windows, Where Pt Is Selected as the Working Electrode and Li Is Used as the Counter and Reference Electrodes^a



^a(a) Schematic diagram of the two-electrode system. (b) CV curve of TMS tested in a two-electrode device, at a scan rate of 1 mV s^{-1} . (c) Schematic diagram of the ameliorated three-electrode system. (d) CV curve of TMS tested in a three-electrode device, at a scan rate of 1 mV s^{-1} .

Theoretically, the two-electrode system in Scheme 1a is feasible. However, when it works, the current goes through the lithium tablet used as the counter electrode; accompanied by that electric current, it has passed through the reference electrode. As a result, the test course is unstable, and the electrochemical window platform shown in Scheme 1b is uneven. By contrast, the three-electrode system in Scheme 1c, where an additional lithium slice serves as the reference electrode, makes the CV curve more smooth and the electrochemical tests more accurate, as shown in Scheme 1d. Thus, all of the following CV tests utilize the three-electrode system.

As is shown in Figure 2, the electrochemical window of three different sulfone electrolytes (1 M LiTFSI in TMS/DMS, EMS/DMS, and EVS/DMS) was 5.2, 5.5, and 4.4 V, respectively. Among the three sulfone solvents, 1 M LiTFSI–EMS/DMS [1:1, (v)] and 1 M LiTFSI–TMS/DMS [1:1, (v)] exhibited higher oxidation decomposition potential, which could be 5.7 and 5.5 V, followed by 1 M LiTFSI–EVS/DMS [1:1, (v)] at 4.1 V. The oxidation potentials of these composite electrolytes reflect oxidation potential of single sulfone solvent. Hence, it should be noted that oxidation resistance ability of these three solvents from high to low is EMS > TMS > EVS, which matches with the theoretical calculation results perfectly. The main factors affecting electrochemical stability are the molecular structures of solvents, the functional polar groups of solvents, and the length of carbon chains in the molecule. Therefore, linear sulfones exhibit better antioxidant ability, strong degree of polarization of functional groups, and short

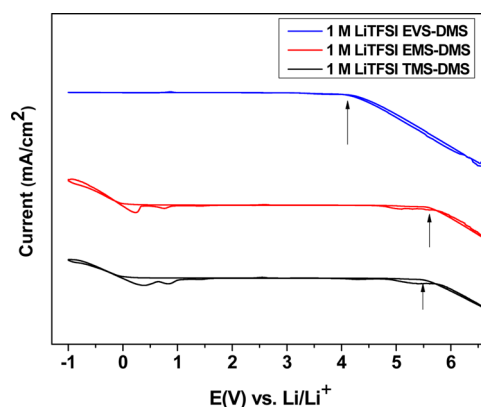


Figure 2. Current–potential curves of LiTFSI in EMS, EVS, and TMS, where DMS was used as cosolvent [1:1, (v)] (Pt as the working electrode and Li as the counter and reference electrodes, at a scan rate of 1 mV s^{-1}).

molecular chains, leading to higher oxidation decomposition voltage.

Combining HOMO energy calculations and electrochemical tests, we concluded that when TMS and EMS are used as the main solvents for electrolytes where lithium salts are added in, the electrochemical window can exceed 5 V. Though the electrochemical stability of EMS is appealing, the melting point of EMS is higher than that of TMS, which would reduce the stability of electrolyte solution after adding lithium salts. Therefore, three different kinds of lithium salts, LiBOB, LiTFSI, and LiPF₆, were added into TMS, DMS, or DES as cosolvent to

test the stability of electrochemical effects of electrolytes, as shown in Figure 3.

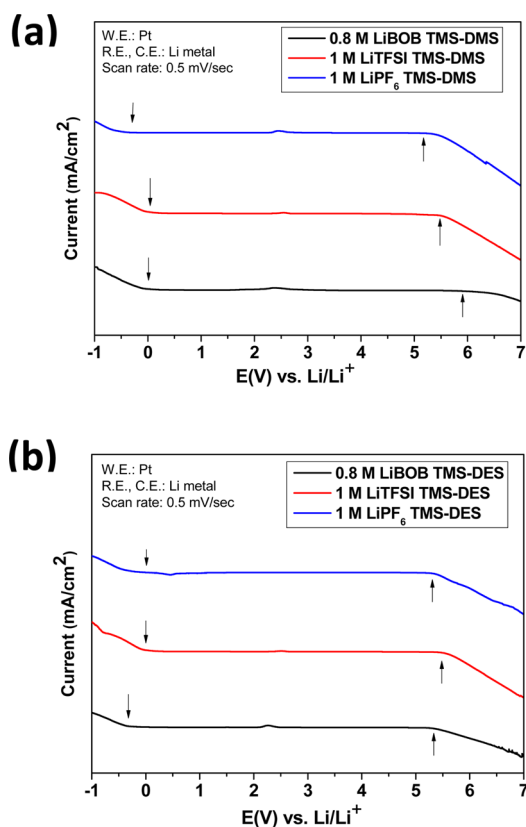


Figure 3. Linear sweep voltammetry determinations of oxidative and reductive stability on Pt for (a) three lithium salts in TMS/DMS [1:1, (v)] and (b) three lithium salts in TMS/DES [1:1, (v)]. (Pt as the working electrode and Li as the counter and reference electrodes, at a scan rate of 0.5 mV s^{-1}).

The oxidation decomposition potential of LiBOB–TMS/DMS is 5.8 V, followed by LiTFSI–TMS/DMS 5.5 V and LiPF₆–TMS/DMS 5.2 V; the reductive decomposition potential is 0.1, 0, and 0.2 V, respectively, as shown in Figure 3a. Thus, LiBOB, LiTFSI, and LiPF₆ in TMS/DMS possess electrochemical windows of 5.7, 5.5, and 5.4 V, respectively. These three electrolytes are all promising because of their high-voltage characteristic. In TMS/DMS, both LiBOB and LiTFSI show good electrochemical stability, while the stability of LiPF₆ is slightly inferior. In addition, it is found that LiPF₆–TMS/DMS electrolytic solution turned yellow gradually after a period of time (shown in Figure 4). Because a small portion of Figure 3b shows the oxidative stability of three kinds of lithium salts in TMS/DES [1:1, (v)], it can be seen that the oxidative decomposition potential of 1 M LiTFSI–TMS/DES is the highest, 5.5 V, and those of 1 M LiPF₆–TMS/DES and 0.8 M LiBOB–TMS/DES are 5.3 V. In addition, the electrochemical window of 0.8 M LiBOB–TMS/DES is 5.5 V, the same as 1.0 M LiTFSI–TMS/DES, and that of 1.0 M LiPF₆–TMS/DES is 5.3 V. So, when DMS is used as cosolvent to adjust TMS, the electrochemical stability would be better than that of TMS/DES.

In addition, it is found that the solutions of LiPF₆–TMS/DMS and LiPF₆–TMS/DES turn orange red or pink gradually after 9 days, as shown in Figure 4. These two solutions are

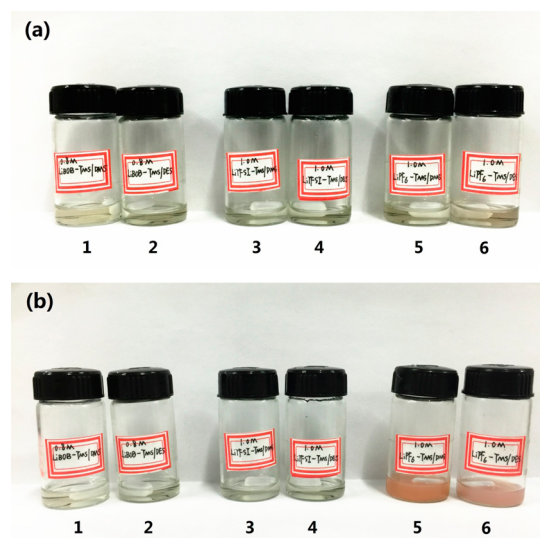


Figure 4. Intuitive views of the sulfone-based electrolytes: (a) freshly prepared, (b) stored in a glovebox for 9 days (no. 1, 0.8 M LiBOB–TMS/DMS; no. 2, 0.8 M LiBOB–TMS/DES; no. 3, 1 M LiTFSI–TMS/DMS; no. 4, 1 M LiTFSI–TMS/DES; no. 5, 1 M LiPF₆–TMS/DMS; no. 6, 1 M LiPF₆–TMS/DES).

transparent when being freshly prepared. This phenomenon is owing to that small amount of impurities in TMS that may cause light and thermal degradation with the effect of LiPF₆ and then change the color of the electrolyte. By contrast, LiBOB–TMS/DMS, LiBOB–TMS/DES, LiTFSI–TMS/DMS, and LiTFSI–TMS/DES are clear and transparent all the time. Hence, it is worth noting that, in TMS/DMS and TMS/DES, both LiBOB and LiTFSI show good stability, while the stability of LiPF₆ is slightly inferior.

3.3. Conductivity Measurements. Conductivities of the sulfone electrolytes were measured from -20 to 60 °C. Ionic conductivity was measured according to the sum of the interface impedance and the ohmic resistance.

The plots in Figure 5 basically conform to the Arrhenius equation.³⁰ With increasing concentration of lithium salts, the conductivities of sulfone electrolytes increase to a maximum value and then decrease. In accordance with the existing theoretical research,³¹ it is demonstrated that the relationship between electrical conductivity and electrolyte concentration is

$$k = \Lambda c / 10^3 \quad (1)$$

$$\Lambda \eta = a \quad (\text{Walden Rules, } a \text{ is a constant}) \quad (2)$$

$$k = \Lambda c / 10^3 = ac / (\eta \times 10^3) \quad (3)$$

where k refers to electrical conductivity, Λ is molar conductivity, c is concentration, and η is viscosity. Formula 3 gives the explanation that the conductivity of electrolytes is mainly affected by the concentration and the viscosity of lithium salts. The viscosity of sulfone electrolytes generally increases with the growing concentration of lithium salts; thus, there will be a maximum value of electrical conductivity as the concentration of lithium salts increases. In TMS/DMS [1:1, (v)], therefore, to obtain the best conductivity, as shown in Figure 5, the concentration of LiBOB is 0.8 M; even at -20 °C, the conductivity of 0.8 M LiBOB–TMS/DMS is $7.92 \times 10^{-4} \text{ S cm}^{-1}$, and the concentration of LiTFSI is 1.0 M, possessing the highest conductivity in TMS/DMS, which could reach $1.03 \times$

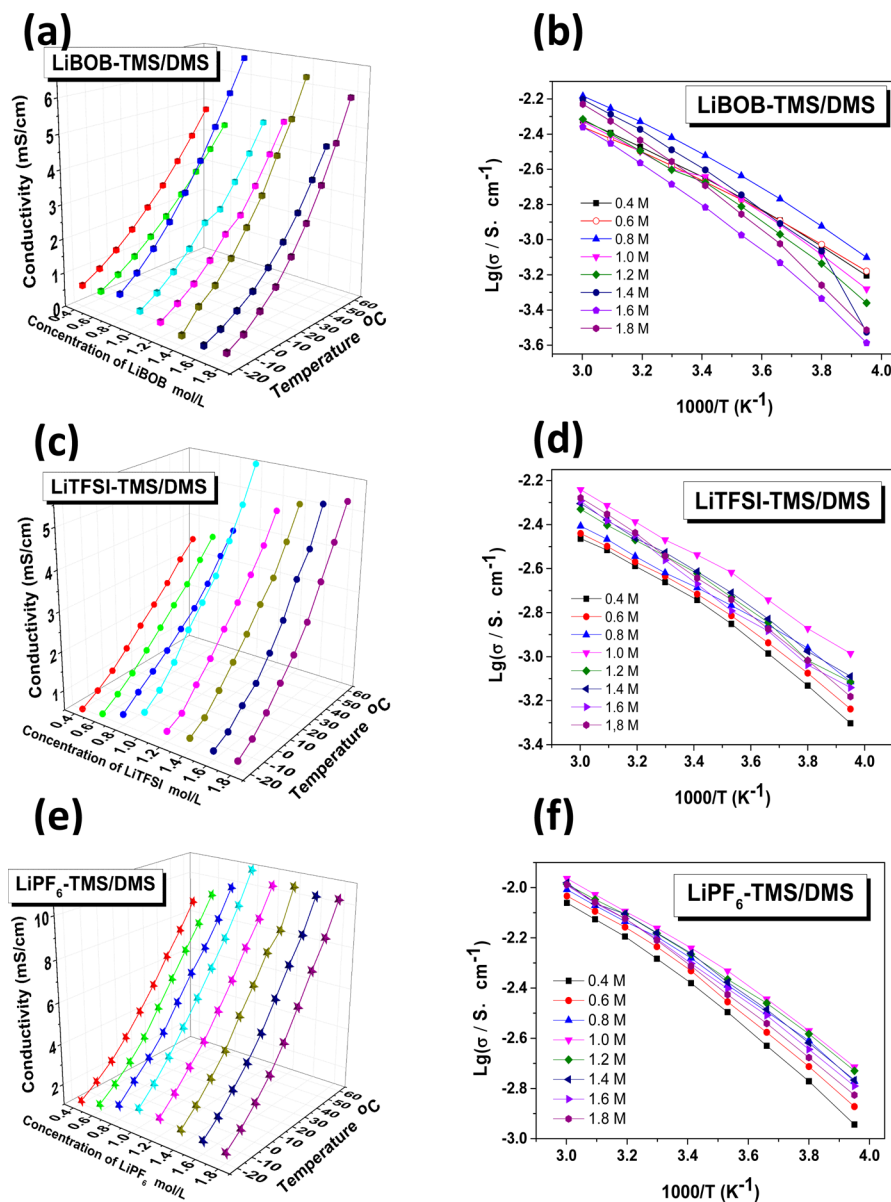


Figure 5. Ionic conductivities for three sulfone-based electrolytes from -20 to 60 $^{\circ}\text{C}$, with different lithium salt concentrations: (a) LiBOB–TMS/DMS, (c) LiTFSI–TMS/DMS, and (e) LiPF₆–TMS/DMS. Arrhenius plots of the temperature dependence for three sulfone-based electrolytes: (b) LiBOB–TMS/DMS, (d) LiTFSI–TMS/DMS, and (f) LiPF₆–TMS/DMS.

10^{-3} S cm^{-1} at -20 $^{\circ}\text{C}$. Also, the conductivity of 1.0 M LiPF₆–TMS/DMS is 1.93×10^{-3} S cm^{-1} at -20 $^{\circ}\text{C}$.

At 60 $^{\circ}\text{C}$, 1.0 M LiPF₆–TMS/DMS [1:1, (v)] shows the highest conductivity 1.09×10^{-2} S cm^{-1} , as shown in Figure 6. From 10 to 30 $^{\circ}\text{C}$, in TMS/DMS [1:1, (v)], the ionic conductivities of LiBOB-based and LiTFSI-based electrolytes are close, and when the temperature is below 10 $^{\circ}\text{C}$, the ionic conductivity of LiTFSI is better than that of LiBOB, whereas at temperatures higher than 30 $^{\circ}\text{C}$, the ionic conductivity of LiBOB is better than that of LiTFSI. The order of the conductivities of lithium salts in TMS/DES [1:1, (v)] from high to low is LiTFSI > LiPF₆ > LiBOB. Table 3 shows numerical values of ionic conductivities of three lithium salts in TMS/DMS [1:1, (v)] and TMS/DES [1:1, (v)] at various temperatures. All these electrolytes possess ionic conductivity ranging from 2.94×10^{-3} S cm^{-1} (0.8 M LiBOB–TMS/DES) to 6.34×10^{-3} S cm^{-1} (1 M LiPF₆–TMS/DMS) at 25 $^{\circ}\text{C}$. No matter in TMS/DMS or in TMS/DES at room temperature, it

is noted that the ionic conductivity of LiPF₆ is better than that of LiBOB, as shown in Table 3. The reason may be that the volume of the BOB[−] group is larger, leading to worse ion association with Li⁺ than that between Li⁺ and PF₆[−]; thus, more Li⁺ ions associate with solvent molecules in LiBOB–TMS/DMS (or LiBOB–TMS/DES), and increases the electrolyte viscosity, causing high activation energy for Li⁺ diffusion. Therefore, the ionic conductivity of LiPF₆ presents better than that of LiBOB.

3.4. ATR-FTIR Analysis. The ATR-FTIR is a useful tool to analyze the interactions between cations and anions in electrolytes, which is delicate to minute variations in molecule structures.³² The antisymmetric stretching vibration of O=S=O in sulfone lies in about 1300 cm^{-1} , and its symmetry vibration band usually appears from 1160 to 1100 cm^{-1} , as shown in Figure 7. While for sulfate solvents DMS and DES the S=O stretching vibration band is near 1200 cm^{-1} , the O–S–O stretching vibration band is usually at 750 – 650 cm^{-1} and the

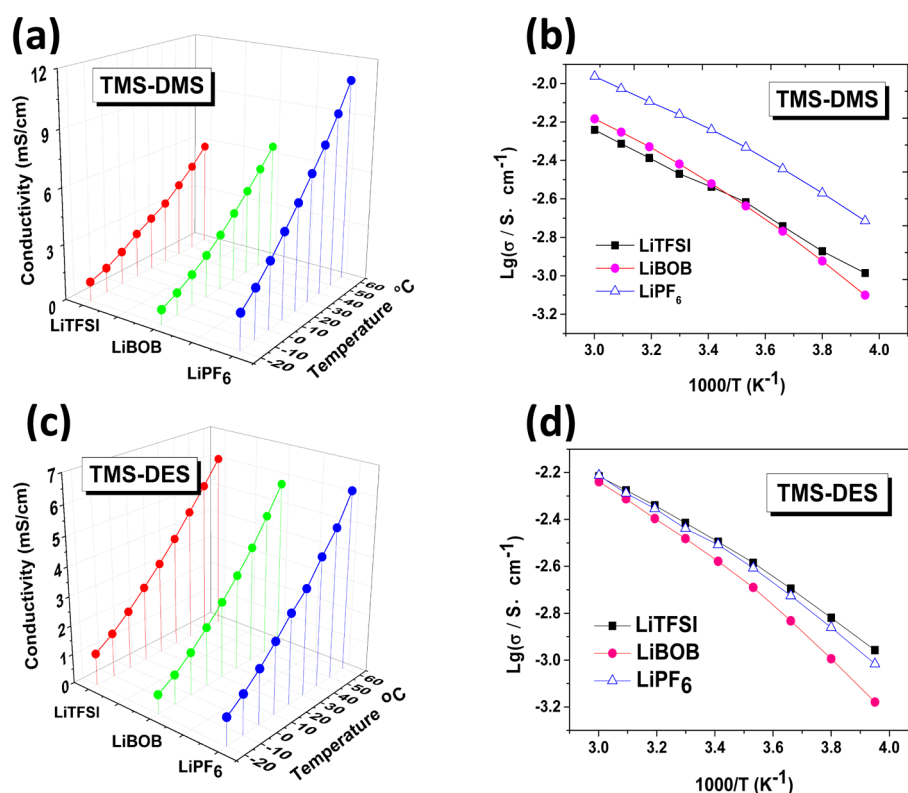


Figure 6. Ionic conductivities for three lithium salts in different sulfone-based solvents, from -20 to 60 °C: (a) TMS/DMS [1:1, (v)] and (c) TMS/DES [1:1, (v)]. Arrhenius plots of the temperature dependence for three lithium salts in (b) TMS/DMS [1:1, (v)] and (d) TMS/DES [1:1, (v)].

Table 3. Ionic Conductivities of High-Voltage Sulfone Electrolytes at Various Temperatures

sulfone solvents	lithium salt	conductivity (10^{-3} S/cm)									
		-20 °C	-10 °C	0 °C	10 °C	20 °C	25 °C	30 °C	40 °C	50 °C	60 °C
TMS/DMS(1:1)	0.8 M LiBOB	0.79	1.19	1.7	2.31	3.01	3.43	3.81	4.69	5.59	6.54
	1 M LiTFSI	1.03	1.34	1.81	2.41	2.9	3.19	3.39	4.1	4.86	5.74
	1 M LiPF ₆	1.93	2.69	3.6	4.66	5.75	6.34	6.9	8.05	9.39	10.88
TMS/DES(1:1)	0.8 M LiBOB	0.66	1.01	1.47	2.04	2.64	2.94	3.3	4.02	4.88	5.77
	1 M LiTFSI	1.1	1.52	2.02	2.6	3.2	3.55	3.85	4.57	5.3	6.08
	1 M LiPF ₆	0.96	1.38	1.88	2.47	3.11	3.28	3.64	4.43	5.15	6.14

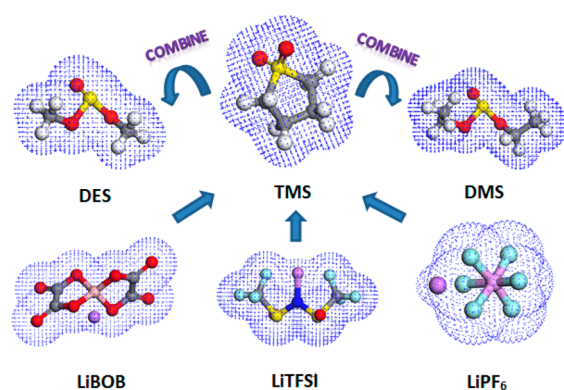
stretching vibration bands of S–O, C–O, and C–C in S–O–C–C lie near 750 – 650 , 1030 – 960 , and 960 – 880 cm^{-1} , respectively. All the vibration modes and corresponding peak positions of two solvent systems added with three lithium salts are listed in Table 4.

LiTFSI–TMS/DMS has one characteristic peak at 614 cm^{-1} , as shown in Figure 7a, curve C; since strong stretching vibration bands of SO_3H and SO_3^- usually appear from 600 to 650 cm^{-1} , reaction between LiTFSI and TMS/DMS may generate SO_3^- (harmonic peak at 614 cm^{-1}), and the increasing intensity of the vibration at 512 cm^{-1} may manifest that there exists alteration on magnitude of dipole moment in the C–S bond in TMS. According to Scheme 2, we can clearly see that there is a O=S=O group in the structure of TMS. The S atom's sp^3 hybridized orbital in TMS consists of two S=O bands, and that orbital in DMS or DES consists of one S=O band in $-\text{SO}_3$. The electron cloud density of O=S=O in TMS is the largest, which contributes to the coordination with 2s empty orbit of Li^+ ions. Hence, it is deduced that sulfone oxygen has a strong coordination with Li^+ ions. In LiTFSI–TMS/DMS, S=O stretch vibration at 1200 cm^{-1} has a red shift to 1186 cm^{-1} , as shown in Figure 7b, curve C. It can be

concluded that Li^+ in LiTFSI coordinates with the S=O bond in the sulfone group and affects the S=O stretching vibration, and this coordination makes the S=O bond lengthen and the bond strength be weaker, resulting in this red shift. The characteristic spectral bands of LiTFSI may at 1059 and 1358 cm^{-1} .

LiPF₆ causes a red shift on the band near 567 cm^{-1} ($-\text{SO}_3^-$ stretch), as shown in Figure 7a, curve D, and 7c, curve D, due to P–F bond in LiPF₆ affecting $-\text{SO}_3^-$ bond-stretching vibration in DMS or DES, leading to the decrease of its wavenumber. Hence, this could be the factor that makes LiPF₆–TMS/DMS conductivity higher than that of LiBOB or LiTFSI in TMS/DMS. A harmonic peak at around 839 cm^{-1} is the characteristic peak of LiPF₆ in TMS/DMS. The characteristic peak of LiPF₆³³ is a harmonic peak at around 846 cm^{-1} ; red shift occurs at 839 cm^{-1} when LiPF₆ is added into TMS/DMS or TMS/DES, as shown in Figure 7b, curve D, and 7c, curve D. Also, we speculate O=S=O in TMS may affect the length of the bond in LiPF₆. LiBOB makes O=S=O symmetry vibration shift red in TMS/DMS at 1100 cm^{-1} . This is because LiBOB has a stable ring lactone structure; at the same time, its structure is similar to TMS and DMS, making it

Scheme 2. Electron Cloud Structures of Lithium Salts and Sulfone Solvents



easier for the lithium salt to dissociate, even easier to form stable sulfone solvents. To some extent, this offers evidence about why LiBOB–TMS/DMS possesses the best electrochemical stability.

Furthermore, the three lithium salts all cause C–S stretching vibration in TMS/DES blue shift at 710 cm^{-1} , as shown in Figure 7c. The addition of lithium salts may shorten the C–S bond length. In addition, LiTFSI may have a strong effect on the S=O stretching vibration since a red shift occurs from 1200 to 1185 cm^{-1} (in Figure 7d, curve C). Therefore, effects of three lithium salts in sulfone solvents are different: LiTFSI and LiPF₆ exert more influence on the molecular vibrations of solvents, while LiBOB relatively keeps the original vibrations of sulfone solvents.

4. CONCLUSIONS

Theoretical calculations of frontier molecular orbital energies of several sulfones suggest that EMS, TMS, and EVS have relatively better oxidation stability. And it is proven experimentally by an electrochemical performance test that oxidation stability of these three sulfones from high to low is EMS, TMS, and EVS, which is in accordance with theoretical calculation results. LiBOB (0.8 M), used as a lithium salt in TMS/DMS [1:1, (v)], could possess the widest electrochemical window of 5.7 V. Besides, to present the best ionic conductivity in TMS/DMS, the concentration of LiBOB is 0.8 M and the concentration of LiTFSI and that of LiPF₆ are 1 M. In addition, 1 M LiPF₆–TMS/DMS [1:1, (v)] has superior ionic conductivity of $6.34 \times 10^{-3}\text{ S cm}^{-1}$ at room temperature. Experimentally, as for 0.8 M LiBOB–TMS/DMS [1:1, (v)], 0.8 M LiBOB–TMS/DES [1:1, (v)], 1.0 M LiTFSI–TMS/DMS [1:1, (v)], 1.0 M LiTFSI–TMS/DES [1:1, (v)], 1.0 M LiPF₆–TMS/DMS [1:1, (v)], and 1.0 M LiPF₆–TMS/DMS [1:1, (v)], the oxidation decomposition potentials of those sulfone electrolytes are all above 5 V, and their electrolyte conductivities at room temperature are more than 3 mS/cm. ATR-FITR spectra offer further explanations about the interaction between lithium salts and sulfone solvents. Because of the addition of LiBOB, LiTFSI, and LiPF₆, the characteristic peaks of the TMS/DMS and TMS/DES functional sulfone groups and sulfonic acid ester groups are red-shifted or blue-shifted, which results in differences in ionic conductivity and electrochemical stability of electrolytes. In summary, we present here a successful demonstration that it would be more efficient and reliable to combine theoretical calculations and experimental tests to determine high-voltage electrolyte solvents. It

indicates that TMS/DMS and TMS/DES are promising sulfone solvents for high-voltage lithium-ion batteries.

AUTHOR INFORMATION

Corresponding Authors

*Phone: (+86)-10-68912528. E-mail: membrane@bit.edu.cn (Y.B.).

*Phone: (+86)-10-68912657. E-mail: chuanwu@bit.edu.cn (C.W.).

Notes

The authors declare no competing financial interest.

ACKNOWLEDGMENTS

This work was supported by the National Basic Research Program of China (No. 2015CB251100), the Program for New Century Excellent Talents in University (NCET-13-0033), the Beijing Co-construction Project (No. 20150939014), and the Beijing Higher Institution Engineering Research Center of Power Battery and Chemical Energy Materials.

REFERENCES

- Christian, M. Driving Change in the Battery Industry. *Nat. Nanotechnol.* **2014**, *9*, 327–328.
- Goodenough, J. B.; Kim, Y. Challenges for Rechargeable Batteries. *J. Power Sources* **2011**, *196*, 6688–6694.
- Bai, Y.; Tang, Y.; Wang, Z.; Jia, Z.; Wu, F.; Wu, C.; Liu, G. Electrochemical Performance of Si/CeO₂/Polyaniline Composites as Anode Materials for Lithium Ion Batteries. *Solid State Ionics* **2015**, *272*, 24–29.
- Xu, K. Nonaqueous Liquid Electrolytes for Lithium-Based Rechargeable Batteries. *Chem. Rev.* **2004**, *104*, 4303–4417.
- Jia, Z.; Yuan, W.; Zhao, H.; Hu, H.; Baker, G. L. Composite Electrolytes Comprised of Poly(ethylene oxide) and Silica Nanoparticles with Grafted Poly(ethylene oxide)-Containing Polymers. *RSC Adv.* **2014**, *4* (77), 41087–41098.
- Hu, H.; Yuan, W.; Lu, L.; Zhao, H.; Jia, Z.; Baker, G. L. Low Glass Transition Temperature Polymer Electrolyte Prepared from Ionic Liquid Grafted Polyethylene Oxide. *J. Polym. Sci., Part A: Polym. Chem.* **2014**, *52* (15), 2104–2110.
- Hu, H.; Yuan, W.; Jia, Z.; Baker, G. L. Ionic Liquid-Based Random Copolymers: A New Type of Polymer Electrolyte with Low Glass Transition Temperature. *RSC Adv.* **2015**, *5* (5), 3135–3140.
- Yang, L.; Ravidel, B.; Lucht, B. L. Electrolyte Reactions with the Surface of High Voltage LiNi_{0.5}Mn_{1.5}O₄ Cathodes for Lithium-Ion Batteries. *Electrochem. Solid-State Lett.* **2010**, *13* (8), A95–A97G.
- Xu, K.; Angell, C. A. Sulfone-Based Electrolytes for Lithium-Ion Batteries. *J. Chem. Soc.* **2002**, *149* (7), A920–A926.
- Sun, X. G.; Angell, C. A. New Sulfone Electrolytes for Rechargeable Lithium Batteries. Part I. Oligoether-Containing Sulfones. *Electrochem. Commun.* **2005**, *7*, 261–266.
- Abouimrane, A.; Belharouak, I.; Amine, K. Sulfone-Based Electrolytes for High-Voltage Li-Ion Batteries. *Electrochem. Commun.* **2009**, *11*, 1073–1076.
- Sedlarikova, M.; Vondrak, J.; Maca, J.; Bartusek, K. Sulfolane as solvent for lithium battery electrolytes. *J. New Mater. Electrochem. Syst.* **2013**, *2*, 65–71.
- Li, S.; Li, B.; Xu, X.; Shi, X.; Zhao, Y.; Mao, L.; Cui, X. Electrochemical Performances of Two Kinds of Electrolytes Based on Lithium Bis(oxalato) Borate and Sulfolane for Advanced Lithium Ion Batteries. *J. Power Sources* **2012**, *209*, 295–300.
- Ping, P.; Wang, Q.; Kong, D.; Zhang, C.; Sun, J.; Chen, C. Dimethyl Sulfoxide as An Additive for Lithiumbis(oxalato)borate/ γ -Butyrolactone Electrolyte To Improve the Performance of Li-Ion Battery. *J. Electroanal. Chem.* **2014**, *731*, 119–127.
- Xing, L. D.; Vatamanu, J.; Borodin, O.; Smith, G. D.; Bedrov, D. Electrode/Electrolyte Interface in Sulfolane-Based Electrolytes for Li

Ion Batteries: A Molecular Dynamics Simulation Study. *J. Phys. Chem. C* **2012**, *116*, 23871–23881.

(16) Lee, S. Y.; Ueno, L.; Angell, C. A. Lithium Salt Solutions in Mixed Sulfone and Sulfone-Carbonate Solvents: A Walden Plot Analysis of the Maximally Conductive Compositions. *J. Phys. Chem. C* **2012**, *116*, 23915–23920.

(17) Cui, X.; Zhang, H.; Li, S.; Zhao, Y.; Mao, L.; Zhao, W.; Li, Y.; Ye, X. Electrochemical Performances of a Novel High-Voltage Electrolyte Based upon Sulfolane and γ -Butyrolactone. *J. Power Sources* **2013**, *240*, 476–485.

(18) Xue, L.; Ueno, K.; Lee, S. Y.; Angell, A. Enhanced Performance of Sulfone-based Electrolytes at Lithium Ion Battery Electrodes, Including the $\text{LiNi}_{0.5}\text{Mn}_{1.5}\text{O}_4$ High Voltage Cathode. *J. Power Sources* **2014**, *262*, 123–128.

(19) Hofmann, A.; Schulz, M.; Indris, S.; Heinzmann, R.; Hanemann, T. Mixtures of Ionic Liquid and Sulfolane as Electrolytes for Li-Ion Batteries. *Electrochim. Acta* **2014**, *147*, 704–711.

(20) Sakaguchi, Y.; Takase, S.; Omote, K.; Asako, Y.; Kimura, K. Sulfonation of Novel Fluorine-Containing Poly(arylene ether nitrile)s for Polymer Electrolyte Membranes. *J. Macromol. Sci., Part A: Pure Appl. Chem.* **2013**, *50*, 879–884.

(21) Bhatt, M. D.; O'Dwyer, C. Recent Progress in Theoretical and Computational Investigations of Li-Ion Battery Materials and Electrolytes. *Phys. Chem. Chem. Phys.* **2015**, *17*, 4799–4844.

(22) Shao, N.; Sun, X.; Dai, S.; Jiang, D. Oxidation Potentials of Functionalized Sulfone Solvents for High-Voltage Li-Ion Batteries: A Computational Study. *J. Phys. Chem. B* **2012**, *116*, 3235–3238.

(23) Rajput, N. N.; Qu, X.; Sa, N.; Burrell, A. K.; Persson, K. A. The Coupling Between Stability and Ion Pair Formation in Magnesium Electrolytes from First-Principles Quantum Mechanics and Classical Molecular Dynamics. *J. Am. Chem. Soc.* **2015**, *137*, 3411–3420.

(24) Wu, F.; Lee, J. T.; Nitta, N.; Kim, H.; Borodin, O.; Yushin, G. Lithium Iodide as a Promising Electrolyte Additive for Lithium-Sulfur Batteries: Mechanisms of Performance Enhancement. *Adv. Mater.* **2015**, *27*, 101–108.

(25) Shao, N.; Sun, X.; Dai, S.; Jiang, D. Electrochemical Windows of Sulfone-Based Electrolytes for High-Voltage Li-Ion Batteries. *J. Phys. Chem. B* **2011**, *115*, 12120–12125.

(26) Frisch, M. J.; Trucks, G. W.; Schlegel, H. B.; Scuseria, G. E.; Robb, M. A.; Cheeseman, J. R.; Scalmani, G.; Barone, V.; Mennucci, B.; Petersson, G. A. *Gaussian 09*; Gaussian, Inc.: Wallingford CT, 2010.

(27) Li, B.; Nie, Z.; Vijayakumar, M.; Li, G.; Liu, J.; Sprenkle, V.; Wang, W. Ambipolar Zinc-Polyiodide Electrolyte for a High-Energy Density Aqueous Redox Flow Battery. *Nat. Commun.* **2015**, *10*, 1–8.

(28) Zhang, X. R.; Pugh, J. K.; Ross, P. N. Computation of Thermodynamic Oxidation Potentials of Organic Solvents Using Density Functional Theory. *J. Electrochem. Soc.* **2001**, *148* (5), E183–E188.

(29) Ue, M.; Murakami, A.; Nakamura, S. J. Anodic Stability of Several Anions Examined by Ab Initio Molecular Orbital and Density Functional Theories. *J. Electrochem. Soc.* **2002**, *149*, A1572–A1577.

(30) Nookala, M.; Kumar, B.; Rodrigues, S. Ionic Conductivity and Ambient Temperature Li Electrode Reaction in Composite Polymer Electrolytes Containing Nanosize Alumina. *J. Power Sources* **2002**, *111*, 165–172.

(31) Pires, J.; Timperman, L.; Jacquemin, J.; Balducci, A.; Anouti, M. Density, Conductivity, Viscosity, and Excess Properties of (Pyrrolidinium Nitrate-Based Protic Ionic Liquid + Propylene Carbonate) Binary Mixture. *J. Chem. Thermodyn.* **2013**, *59*, 10–19.

(32) Shi, F.; Ross, P. N.; Zhao, H.; Liu, G.; Somorjai, G. A.; Komvopoulos, K. A Catalytic Path for Electrolyte Reduction in Lithium-Ion Cells Revealed by in Situ Attenuated Total Reflection-Fourier Transform Infrared Spectroscopy. *J. Am. Chem. Soc.* **2015**, *137*, 3181–3184.

(33) Wu, C.; Bai, Y.; Wu, F. Fourier-Transform Infrared Spectroscopic Studies on the Solid Electrolyte Interphase Formed on Li-Doped Spinel $\text{Li}_{1.05}\text{Mn}_{1.96}\text{O}_4$ Cathode. *J. Power Sources* **2009**, *189*, 89–94.